ARTICLE

https://doi.org/10.1590/2317-4889202020190031

BJGEO
Brazilian Journal of Geology

Method to complete flow rate data in automatic fluviometric stations in the karst system of Lagoa Santa area, MG, Brazil

Rodrigo Sérgio de Paula[1]*, Leila Nunes Menegasse Velásquez[1]

Abstract

Data acquisition by automatic monitoring allows obtaining a large number of data, supporting a better understanding of the monitored region. The use of automated discharge measurement enables a better understanding of floods, the relationship between surface and ground-water flow rate values, and aquifer recharge. However, automatic instruments processing and storage may fail, leading to missing values in some intervals of the recorded time series. These missing values may be replaced by estimates from the regional flow rate or other statistical approximations. For evolved karst systems, however, those techniques may not be adequate due to their rapid discharge responses to rainfall. The aim of this paper is to develop a method able to estimate fluviometric monitoring missing values, based on time series correlation for correlated data. These estimates were obtained from automated monitoring through pressure transducers in 6 streams in a region of approximately 505 km^2, predominantly covered by the carbonate and metapellitic Neoproterozoic rocks of the Bambuí Group. The proposed method is composed of four sequential steps: computing the streamflow-data autocorrelation and the cross-correlation of pluviometry with the flow rate; calculating the precipitation fraction that directly contributes to the discharge; fitting of a linear relationship between pluviometry and the monitored daily discharge, to calculate discharge values on days when automatic measurements failed; and approximation of the calculated and monitored discharge values, using a number of statistical criteria. The results show the maturity of the karst aquifer system, with fast ground-water flow and low storage, well-calibrated stage-discharge rating curves for the 2016/2017 hydrological year and that the values estimated by proposed methodology present a deviation of less than 9% over the monitored data.

KEYWORDS: karst-fissural aquifer; cross-correlation; flow rate autocorrelation; fluvial discharge monitoring; hydrological data completion.

INTRODUCTION

The study area has 505 km^2 and it is in the northern zone of the metropolitan region of Belo Horizonte, Minas Gerais, covering the entire region named Environmental Protection Area (*Área de Proteção Ambiental* — APA) of Lagoa Santa Karst and its surroundings. This area is undergoing rapid urban and industrial expansion, which leads to a substantial increase in water demand. Therefore, the assessment of the regional hydrological basins flow is fundamental for the understanding and sound management of its water system.

In order to perform the streams fluviometric analysis, pressure transducers were installed. The pressure is measured every 15 minutes and then averaged as daily discharge data. Automated monitoring, however, may present flaws in data collection and storage, leading to missing values in the recorded time series. Typically, data failure completion involves one of the following methods.

Existing data failure completion methods typically use:

- either interpolators or percentile methods to fill gaps at time intervals greater than 24 hours;
- long series of data to complete minor failures;
- average discharge regionalization methods and permanence curve;
- correlations of physiographies between similar basins.

As described by Obregon *et al.* (1999), the discharge regionalization method, as well as the permanence curve, are the main hydrological functions to complete monitoring flaws.

Freund and Wilson (1998) used the Quadratic Least Square Regression model to measure the correlation of hydrological data between fluviometric stations. Barbosa (2004) used discharge regionalization to fill flow rate data failures in the southern region of Minas Gerais State, Brazil. Collischonn and Tassi (2008) proposed the transfer of flow rate data between basins and the establishment of a linear relationship between the discharge and drainage areas. Tamiosso *et al.* (2013) used the classical Manning methodology to fill defects in flow rate data failures. However, in well-developed karstic environments, the heterogeneity and anisotropy of the system indicate specific characteristics for different basins and an almost instantaneous flow rate response to rainfall events. The existing methodologies are not fully adequate for karst environment and there is a lack of limited specific studies about this theme in karst regions. The author presents a solution to manage the presence of missing values in time lapses due to acquisition failures in automatized fluviometric monitoring.

[1]Universidade Federal de Minas Gerais – Belo Horizonte (MG), Brazil.
E-mails: rodrigo.spdm@yahoo.com.br, menegase@yahoo.com.br

*Corresponding author.

© 2020 The authors. This is an open access article distributed under the terms of the Creative Commons license.

The proposed method was applied to a data set from the northern zone of the metropolitan region of Belo Horizonte, Minas Gerais, covering the entire region named APA of Lagoa Santa Karst and its surroundings.

The study area is represented from base to top by the Belo Horizonte Gnassic-Granitic-Migmatitic Complex, overlapped by the rocks of Sete Lagoas and Serra de Santa Helena formations, which are part of the Bambuí Group.

The carbonate rocks of the Sete Lagoas Formation (Bambuí Group) encompasses the majority of the area. Over this zone, a typically karstic landscape developed through chemical dissolution along fractures, faults, bedding planes, and lithological contact, which resulted in swallow holes, depressions, conduits, caves, polje, and other morphological features. Such aspects control most of the direct and fast aquifer system recharge, conduction and discharge in surgences and resurgences. They express an evolved terrain in which drainages are predominantly controlled by groundwater, thus exhibiting a strong interaction with each other.

Therefore, a distinctive diversity is generated for this kind of terrain characterized by the easy interaction between surface and underground environment, mostly promoted by water in the mentioned morphological structures considering the qualitative and quantitative fragility of carbonate systems, because of the heterogeneity and rapid response to pluviometric events with a close relationship between surface and groundwater, the development of a methodology that can correlate daily rainfall events is necessary in order to complete the missing values in a daily discharge series for karst environments.

PHYSICAL CHARACTERISTICS OF THE STUDY AREA

The area has approximately 505 km^2 and it is located 35 km north of the city of Belo Horizonte, in the state of Minas Gerais, Brazil. It encompasses, partially or fully, the municipalities of Lagoa Santa, Vespasiano, São José da Lapa, Funilândia, Confins, Matozinhos, Pedro Leopoldo, and Prudente de Morais. It also entirely covers the region called APA Karst of Lagoa Santa and its surroundings (Fig. 1).

Geologically, the western and southern limits of the study area comprise the Belo Horizonte Gnassic-Granitic-Migmatitic Complex, covered by the Neoproterozoic sediments of the Bambuí Group (Fig. 2).

The Bambui group consists of the carbonates of the Sete Lagoas Formation, composed of, from the bottom to the top: Pedro Leopoldo Member, which is predominantly constituted by impure calcilutites (usually fine-grained and light-colored); and Lagoa Santa Member, constituted by pure dark-colored coarse-grained calcarenites. The basal Member is mainly distributed in the eastern region of the area and it is in contact with the crystalline rocks in the southwest portion of the area.

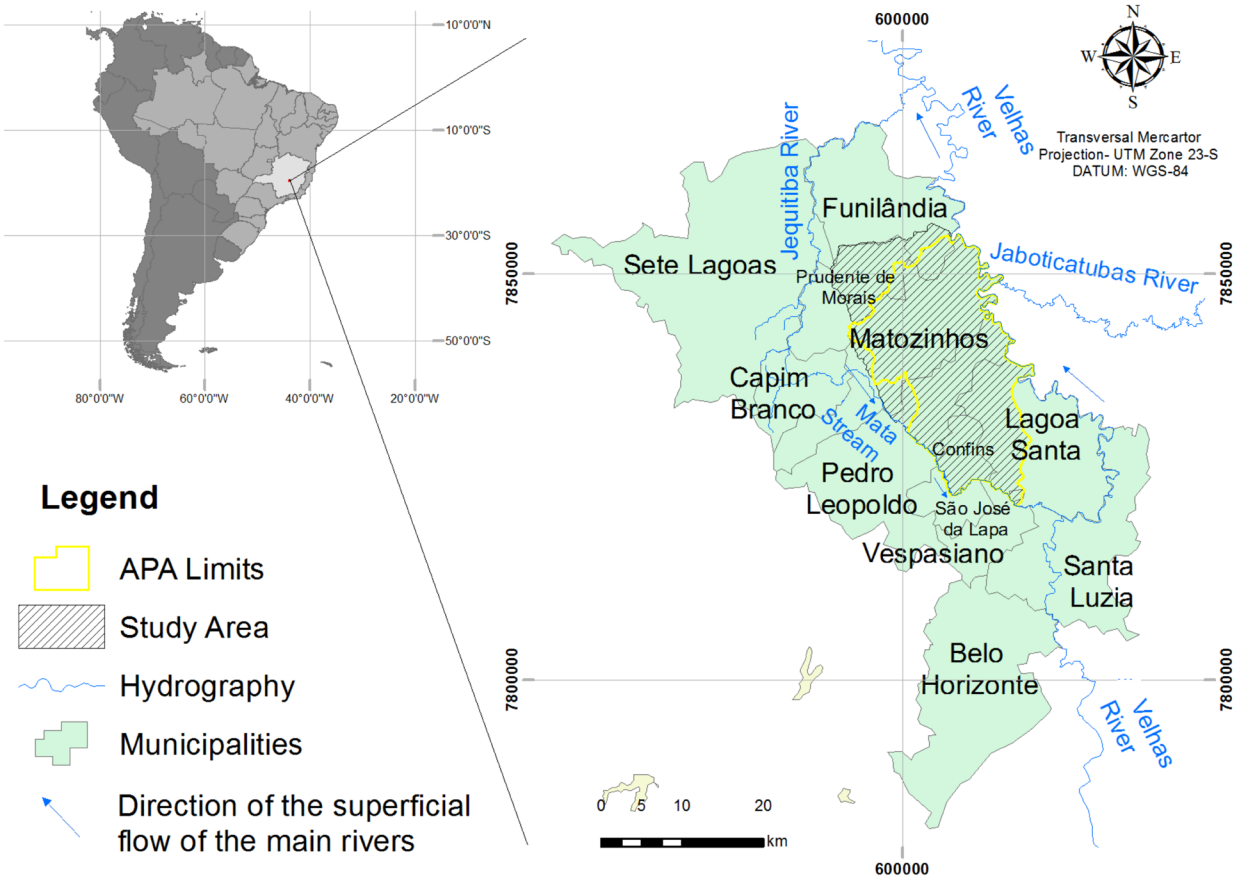

Figure 1. Location Map of the study area, highlighting Environmental Protection Area (*Área de Proteção Ambiental* – APA) – Lagoa Santa Karst (yellow).

On the other hand, the upper Member comprehends more than 60% of the area, distributed from the center to the borders (Fig. 2).

The weathered metapelitic sediments of the Serra de Santa Helena Formation overlap that sequence, located in the eastern portion of the area and, to a lesser extent, to the north and upstream of the Palmeiras stream basin (Fig. 2).

The Cenozoic covers, represented by alluviums on the stream margins and dendritic lateritic covers (Fig. 2), include the pelito-carbonate sequence of the Sete Lagoas and Santa Helena Formation.

As described by Pessoa (2005), the crystalline basement can be found in lower stage-discharge from west to east, and the margins of the Velhas river are its deepest regions. The thickness

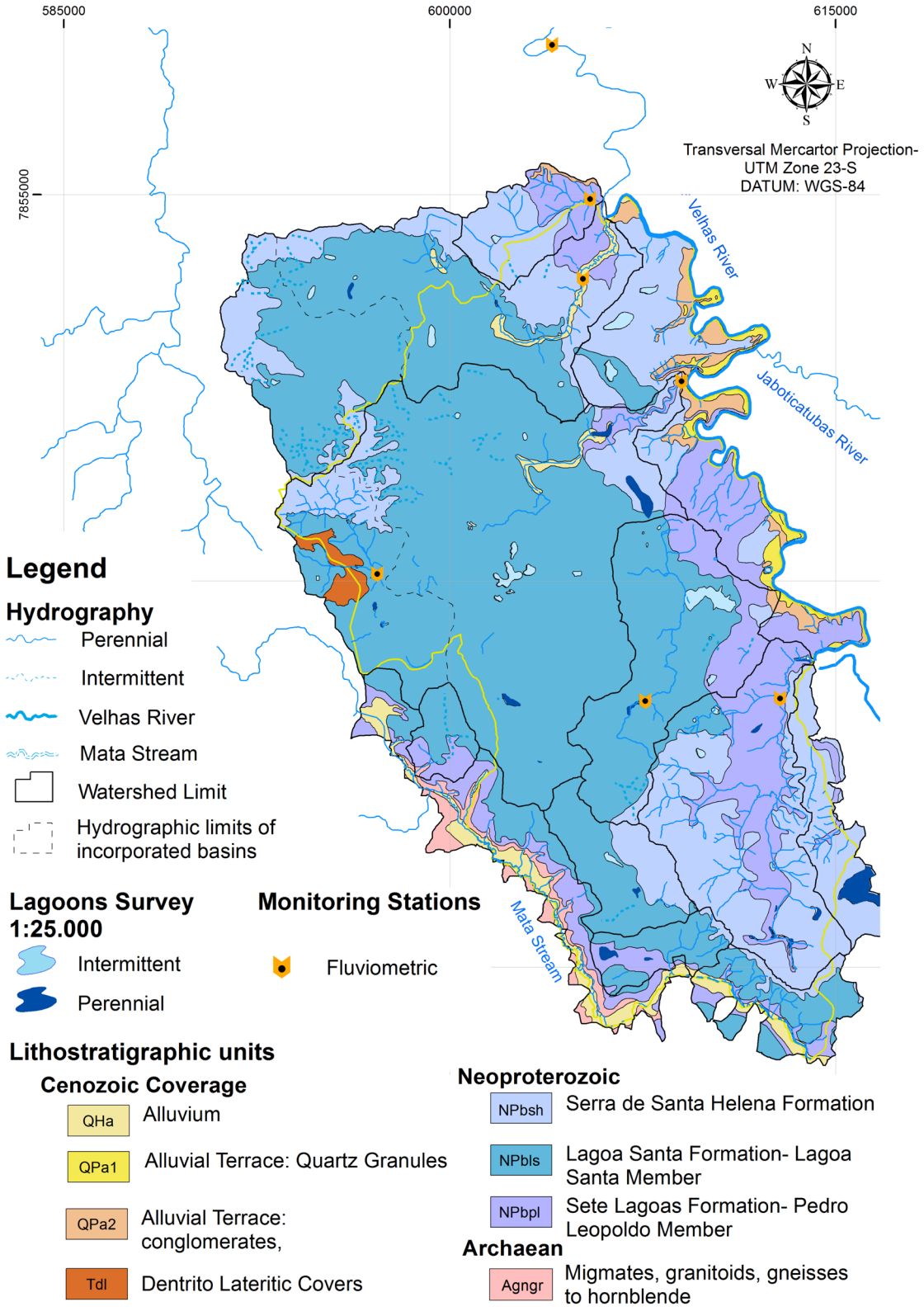

Figure 2. Geological Map (adapted from Ribeiro *et al.* 2003) emphasizing the monitored fluviometric stations.

of the sedimentary basin varies from tens to hundreds of meters as it approaches the limits of the area. Paula (2019) describes average soil thicknesses ranging from 50 to more than 100 m in some regions. Galvão *et al.* (2016), through tubular wells profiles, states that, in regions near the eastern boundary of the area (regions near the Velhas river), the basin thickness is greater than 300 meters.

Structurally, the contacts between the members of the Sete Lagoas Formation are abrupt and discordant. On the other hand, the top and bottom contacts of this geological unit are tectonic, represented by sub-horizontal shear zones, frequently followed by basal displacement flaws and kinematic indicators of reverse movement (Ribeiro *et al.* 2003).

The rupture deformation process that occurred in the zone generated an intense fracture system, which facilitates the aquifer recharge. It is also responsible for the conduction of ground-water flow, either through the fractures themselves or through their dissolution by the action of water and formation of conduits.

The hydrogeological context of the region is represented by the carbonate aquifer of the Sete Lagoas Formation, the main hydrogeological unit, which is deposited directly over the crystalline aquifer formed by the Belo Horizonte Complex and partially covered by the aquitard formed by the pelitic sediments of the Santa Helena Formation and Cenozoic covers.

The gneiss-granite basement represents a low potential fissural aquifer (Vieira *et al.* 1998). Its hydrogeological interaction with the limestone of the formation above (Sete Lagoas Formation) is still not well known. The groundwater flow direction, however, is known to be sub-parallel toward the Velhas river (Andrade and Amorim 2018).

The limestones of the Sete Lagoas Formation constitute the main aquifer unit in the area, with thickness ranging from few meters up to more than 250 m. As stated by Vieira *et al.* (1998), the Lagoa Santa upper Member presents higher water potential if compared to the Pedro Leopoldo Member. This potential is based on the degree of fracture, specific capacity measured in the region's tubular wells, and other parameters. Paula and Velásquez (2019) pointed out the importance of exposed and fractured carbonate massif zones with aquifer recharge, reaching average values for the area of 119 mm for the hydrological year 2016/2017. Ribeiro *et al.* (2019) describe how the groundwater flow of the region is influenced by horizontal planes and eastward fractures.

The metapelites of the Serra de Santa Helena Formation act as aquitards or poor aquifers. The former acts locally as recharge regions for the inferior carbonate aquifers (Pessoa 2005).

The hydrography of the area is represented by the watershed of the Velhas river, being flanked in its northeastern and eastern portions by the same river, which acts as the base level, with heights from 630 to 660 m. To the southwest and west, the Mata stream borders the region, which is a tributary of the Velhas river, located on the right margin (Fig. 3).

Within the area, there are six watersheds that directly or indirectly drain more than 90% of the study area into the Velhas river, through the Palmeiras, Gordura, Jaguara, Samambaia, Flor, and Jaque streams. The fluviometric stations are placed between 1 and 2 km downstream from the meeting of those streams with the Velhas river, ensuring the maximum discharge flow rate from these points. It is worth mentioning that the Palmeiras stream emerges directly into a sink, and its monitoring point is located less than 1 km from that sink. Additionally, the Samambaia stream monitoring point was installed in the middle portion of the basin, due to legal constraints. However, the chosen point represents more than 80% of the total discharge flow rate of this water body (Paula 2019).

The Palmeiras stream flows into a swallow hole and resurfaces after 2.5 km in one of the Jaguara springs (Auler 1994), from where it flows superficially to the Velhas river.

The other streams drain superficially to the left bank of the Velhas river, except for the Samambaia stream, which is entirely drained by a swallow hole, 3 km in a straight line from the left bank of Velhas river. Its resurgence is still unknown.

The residual flow rate of some of the analyzed drainages is affected by several catchments and water abstractions for irrigation and animal watering, drying up during the dry season, when its use is more intense. An important dam located upstream regulates part of the Samambaia stream residual volume.

The streams flow predominantly over karst terrain, except for the Jaque and Flor streams, which partially drain over the metapelites. The physical characteristics of each drainage are described in Table 1. Small marginal basins to the Velhas river and Mata steam flow over covering sediments.

In the basins located entirely above the limestones, the occurrence of low drainage density, without significant tributaries, with the predominance of only first and second order drainages and the concordant orientations of the streams (Fig. 3 and Tab. 1) show a well-evolved karst controlled by tectonics.

The average annual precipitation values, based on the years from 1980 to 2017, of the pluviometric stations that surround the area Lagoa Santa (1943049), Vespasiano (1943049), Pedro Leopoldo (1944009), and Sete Lagoas (OMM: 8670), present a historical average of 1,258.8 mm spread over 93.7 days. There are two well-defined seasons, a dry one from April to September and a rainy one from October to March, which accounts for approximately 90% of total rainfall.

The climatic water balance of the area performed for the same hydrological year of this study (Oct/2016 to Sep/2017) allowed obtaining actual evapotranspiration (AET) of 750 mm (74%), potential evapotranspiration (PET) of 895 mm, water surplus (WS) of 260 mm (26%), and water deficit (WD) of 145 mm, for a precipitation of 1,010 mm recorded at Lagoa Santa station (Paula and Velásquez 2019).

The pluviometric data of Lagoa Santa station from 1980 to 2017 have an average of 1,190 mm, 18% higher than the values monitored in the hydrological year 2016/2017 (Paula 2019). However, this same author shows that the stream discharge monitored in the hydrological year of study remains with adherence of 98% compared to the values monitored by Auler (1994) during the dry period. Therefore, despite various drought stages as well as anthropic interference, the groundwater contribution to this studied hydrographic system remains unchanged.

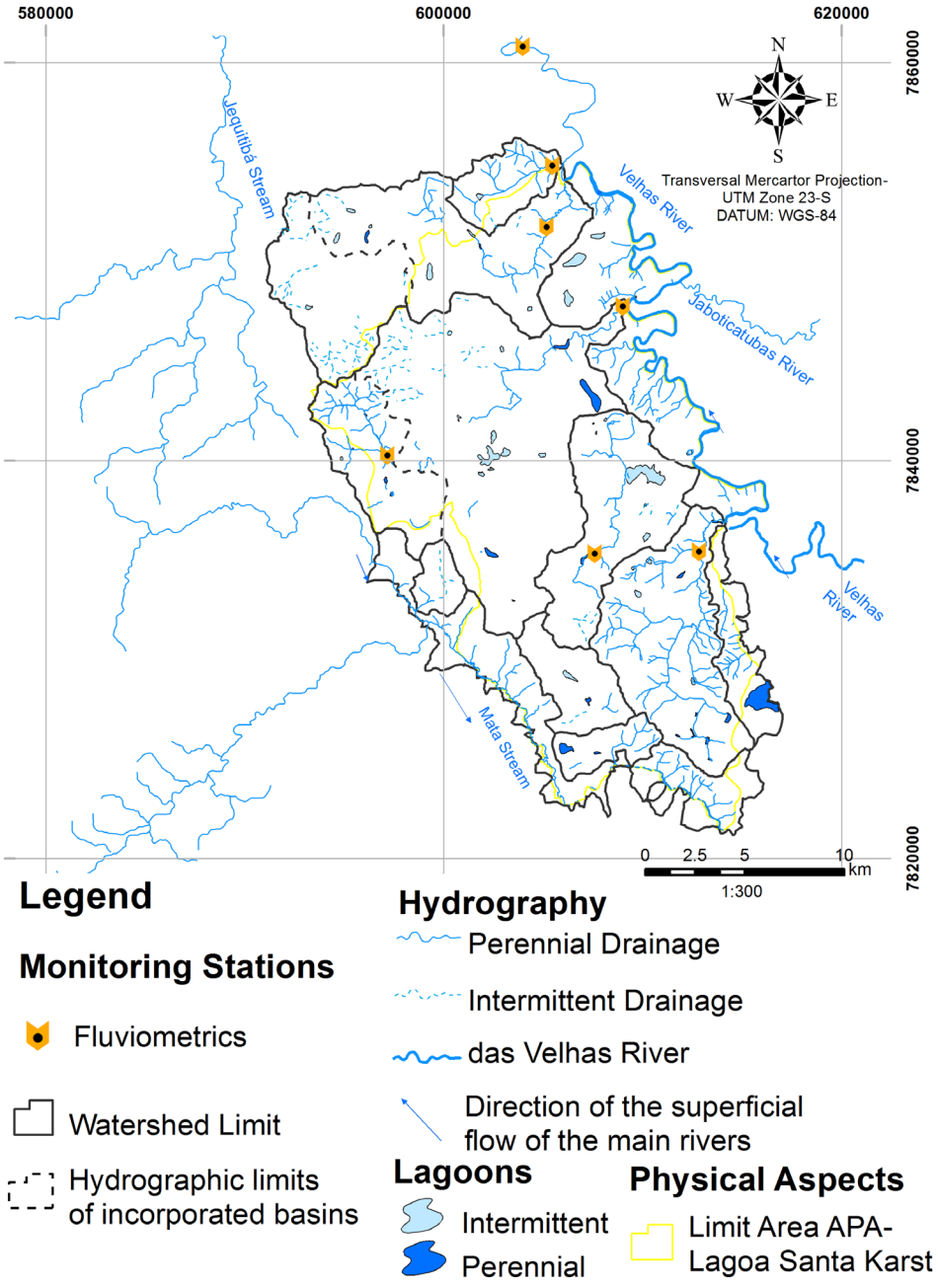

Figure 3. Hydrographic map highlighting the fluviometric monitoring points. In yellow, the APA (Environmental Protection Area) limit area, Lagoa Santa Karst.

Table 1. Physical and lithological characteristics of monitored watersheds.

Basins	Area (km²)	Stream Length (km)	Drainage Direction	Lithology
Flor	16	5.0	SW/NE	Pelite – Limestone
Palmeira	31	6.0	NW/SE	Limestone
Gordura	39	14.0	SW/NE	Limestone
Samambaia	48	9.0	SW/NE	Limestone
Jaque	59	17.0	S/N	Pelite – Limestone
Jaguara	125	14.0	SW/NE	Limestone

MATERIALS AND METHODS

The analyzed data correspond to the monitoring performed from October 2016 to September 2017, equivalent to a regional hydrological year at Lagoa Santa station, which has more than 50% of influence on the evaluated area (Paula and Velásquez 2019).

The pluviometry used for each basin was the one corresponding to the most influential pluviometric station out of four pluviometric stations that surround the area. Paula and Veslásquez (2019) carried out a study in the region which verified, from the Thiessen distribution map, the pluviometric influence of each station on the watersheds, namely: Lagoa

Santa (1943049) — Samambaia Basin, Vespasiano (1943049) and Lagoa Santa (1943049) — Jaque Basin, Pedro Leopoldo (1944009) — Jaguara and Palmeiras, and Sete Lagoas Basins (OMM: 8670) — Gordura, Flor, and Velhas river Basins.

The streamstages were obtained by pressure transducers (*Solinst and Schlumberger*) installed in six streams (Tab. 1). They were calibrated by barometric pressure transducers to obtain the correct water column on the transducer, later converted into water-level coordinates or stages.

Discharge measurements were carried out with conventional current-meters on a bi-monthly basis during the monitoring period.

The stage-discharge rating curves relate the height of the water column of a given course (stage) to its discharge. To make the curve, it is necessary to simultaneously measure the discharge of a stream and its stage, during both the dry and rainy periods, widely representing the fluviometric variation of the water body.

The discharge-stage ratio can be calculated graphically, mathematically or by calibration table. In this work, the international graphical flow rate h/Q is used (Eq. 1):

$$Q = a(h\text{-}h_0)^b \quad (1)$$

Where:
h = the stage height measured for a certain monitored discharge Q;
h_0, = the level at which the flow rate is zero,
a and b = linear constants determined for the location.

To determine the fitting parameters from the univocal relation of the pairs (Q, h), the expression must be linearized, determining a and b by linear regression and h_0 by trial and error (Zahed Filho *et al.* 2001), the SOLVER tool of Excel 2016, which searches for linearization (Q, h) to obtain the smallest possible error for data value h_0, was used in this step.

The discharge-stage rating curve remains valid as long as the physical characteristics of the stream remain close to those of the period in which the data were collected, and the percentage deviations between the analyzed years are less than 10% (Piscoya *et al.* 2013).

The effect of rainfalls on discharge variation was evaluated by the pluviometry-autocorrelation function of and cross–correction between those two variables. The autocorrelation function (Eqs. 2 and 3) (Ferrari and Karmann 2008) measures the linear relationship or the dependency between a series and its lag values, that is, the duration time of the event. Ferrari and Karmann (2008) describe that, for a karst system, the time required for memory loss from initial conditions is between 0.1 and 0.2 for $r(k)$. If such values are found in short time intervals, this indicates an active and well–developed karstic system with little storage.

$$r(k) = \frac{C(k)}{C(0)} \quad (2)$$

$$C(k) = \frac{1}{n} \sum_{t=1}^{n-k} (x_t - \bar{x})(x_{t+k} - \bar{x}) \quad (3)$$

In these equations:
r = the autocorrelation coefficient;
k = the lag time;
C = the autocorrelation of the series;
$C(0)$ = the correlation in k equal to zero, in the length of the series;
x_t = the observed value.
$\bar{x}$ = the average of the observed values.

The cross-correlation function (Eqs. 4 and 5) measures the relationship between two series, in this case, precipitation and water level, and the possible causal relationship between them (Ferrari and Karmann 2008). Understanding the delays between the inflows and outflows in the karstic aquifer is useful for estimating a particle travel time through the system. For $rxy(k) > 0$ while $k > 0$, the input influences the output. If the symmetric function is centered at k = 0, both variables x and y respond to another independent signal and, hence, there is no influence of the input on the output. The delay index k (days) is defined by displacement time between $k = 0$ and k, where $rxy(k)$ is between 0.1 and 0.2.

$$r_{xy}(k) = \frac{C_{xy}(k)}{\sigma_x \sigma_y} \quad (4)$$

$$C_{xy}(k) = \frac{1}{n} \sum_{t=1}^{n-k} (x_t - \bar{x})(y_{t+k} - \bar{y}) \quad (5)$$

Where:
r_{xy} = the correlation coefficient;
k = the time (days) for the discharge to respond to a precipitation event;
C_{xy} = the cross correlogram;
σ_x, σ_y = the standard deviations of the two-time series;
C = the autocorrelation of the series, n the length of the series;
x_t = the value of an observed variable;
$\bar{x}$ = the average of these observed values;
y_t = the value of an observed variable;
$\bar{y}$ = the average of these observed values.

Graphs were plotted, using flow rate data, to represent the time series of flow rate per day for each water body.

In the area of this study, where the response to rainfall events is almost instantaneous, methods that do not correlate daily pluviometric events with instantaneous flow rate would not represent the behavior of the region. Hence the necessity of developing a methodology to directly correlate a complete data series (rainfall) with one that is missing values (flow rate), in order to obtain the effect of pluviometry on the flow rate, enabling completion of the missing curve data. The method is composed of the following four steps:

The first step consisted of performing the autocorrelation of the flow rate time series (Eq. 3), in order to assess whether such data were correlatable, which can be verified when the autocorrelation coefficient tends to range from 0.1 to 0.2, from which the memory loss of the event occurs. Furthermore, at this stage, the cross-correlation (Eq. 5) between precipitation

and flow rate was performed to calculate the time k in days that the flow rate takes to respond to a rainfall event.

Secondly, the portion of the pluviometry which directly influences the flow rate of the water body (Eqs. 6 and 7) Should be determined. To accomplish this goal, AET was calculated using the Thornthwaite method (1948), and this value was then subtracted from the annual pluviometric total. AET calculations were performed using spreadsheets provided by Rolim *et al.* (1998).

$$Pi_n = P_{(n-k)}\,[(P_a - AET)/P_a)] \quad for\ P \neq 0 \tag{6}$$

$$Pi_n = P_{i(n-1)}\,s \quad for\ P = 0 \tag{7}$$

Pi_n (mm) = the portion of rainfall that effectively contributes to flow rate,
P (mm) = daily pluviometry;
P_a = total annual rainfall;
n = any day of the calendar year;
k (days) = delay time between flow rate response and precipitation event;
AET (mm) = the actual evapotranspiration;
s = the estimated surface runoff reduction, determined according to Equation 8.

$$s = \frac{Q_{(n+1)}}{Q_n} \tag{8}$$

Where:
Q (m^3/s) = the monitored flow rate;
n (day) = a day of the calendar year.

The factor s is calculated in the period when there are no rainfall events in order to evaluate the natural reduction of the flow rate without rainfall inputs.

To calculate the portion of daily rainfall that effectively contributes to the stream flow rate (Pi), it was assumed the same annual ratio obtained between these parameters (Eq. 6).

The purpose of the third step was to construct a linear relationship between pluviometry (P) and monitored daily flow rate (Q) by obtaining Equation 9, based on the linearization of the three values (maximum, average, and minimum) of daily precipitation and the three values (minimum, average, and maximum) of the monitored daily flow rate (m^3/s).

$$Q = aP + b \tag{9}$$

Where:
Q (m^3/s) = the daily monitored flow rate;
P (mm) = the daily pluviometry;
a and b = respectively, the angular and linear coefficients obtained graphically.

When P is correlatable to Pi (Eqs. 6 and 7) and Q is correlatable to P (Eq. 5), Q is also correlatable to the calculated flow rate (q) that is influenced by P_i (Eq. 10).

$$q = aP_i + b \tag{10}$$

Since q is the calculated daily flow rate, P_i (mm) is the portion of the daily rainfall that effectively contributes to the discharge in all days of the hydrological year; a and b are, respectively, the angular and linear coefficients obtained graphically above.

Then, by using Equation 10, the flow rate values can be obtained on the days when automatic measurements failed.

The fourth and last step focused on calculating the daily standard deviation of the monitored and calculated flow rate – $\sigma_n\,(Q,q)$ aiming to obtain an estimate q of the monitored values Q. The average standard deviation of all daily data $\bar{\sigma}(Q)$ is used on days in which measurements of Q are not available.

The resulting corrected flow rate qc (m^3/s) for each day of the calendar year can then be approximated according to Equations 11 and 12.

$$qc_n = q_{(n)} \pm \sigma_n \quad when\ Q \neq 0 \tag{11}$$

$$qc_n = q_{(n)} \pm \bar{\sigma} \quad when\ Q = 0 \tag{12}$$

Where:
qc (m^3/s) = the resulting daily flow;
q = the calculated flow;
σ = the standard deviation of monitored and calculated flow rates;
$\bar{\sigma}$ = the average standard deviation of monitored flow data;
n = a day of the calendar year.

The ± sign varies according to the rainy or dry season, the standard deviation being added in the rainy season and subtracted in the dry period. In order to approximate the calculated rating curve of the resulting daily flow rate to the monitored rating curve, the sum of the standard deviation in the rainy season tends to correct the effect of the storage caused by consecutive rain events. Additionally, the subtraction of the standard deviation in the dry season tends to restrict flow rate to the baseflow.

RESULTS AND DISCUSSION

Rating curve

The discharge values measured in the field were plotted next to those calculated using the rating curves (Figs. 4A–4G), aiming to obtain the adhesion between both curves. For a better graphical representativeness, the data were presented through values in m^3/h.

The proportional difference between the sum of the monitored values minus the calculated values was less than 10%, considered a good adherence between the curves. The characteristic curves of the Gordura, Jaguara, Samambaia, and Jaque streams presented excellent adherence with root mean squared (RMS) of less than 10% of the average streams discharge. The characteristic curves for the Velhas river, Flor and Palmeiras streams presented larger deviations, requiring refinements of points and greater data acquisition.

Time series analysis

To identify the maturity level of the karstic system and the relative storage capacity of the aquifer system, the flow

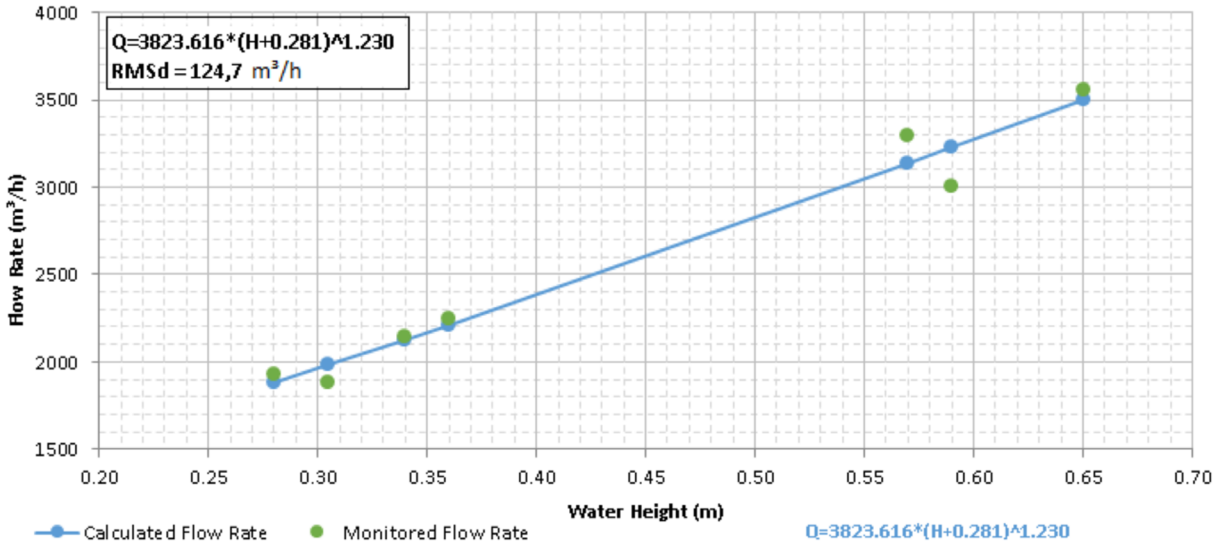

Figure 4A. Rating curve of Gordura stream: calculated and monitored discharge.

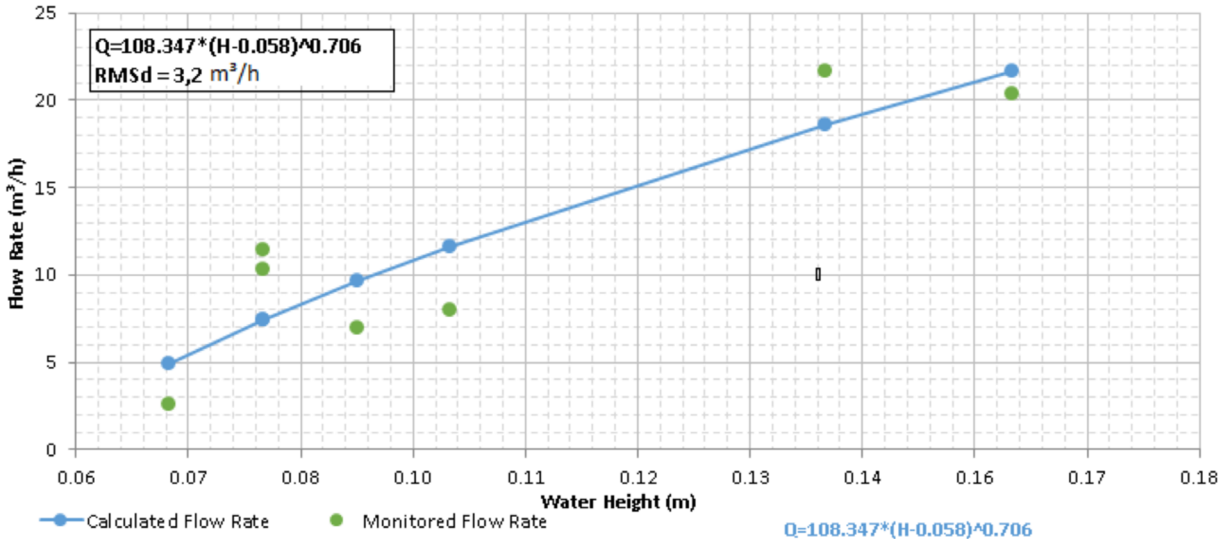

Figure 4B. Rating curve of Flor stream: calculated and monitored discharge.

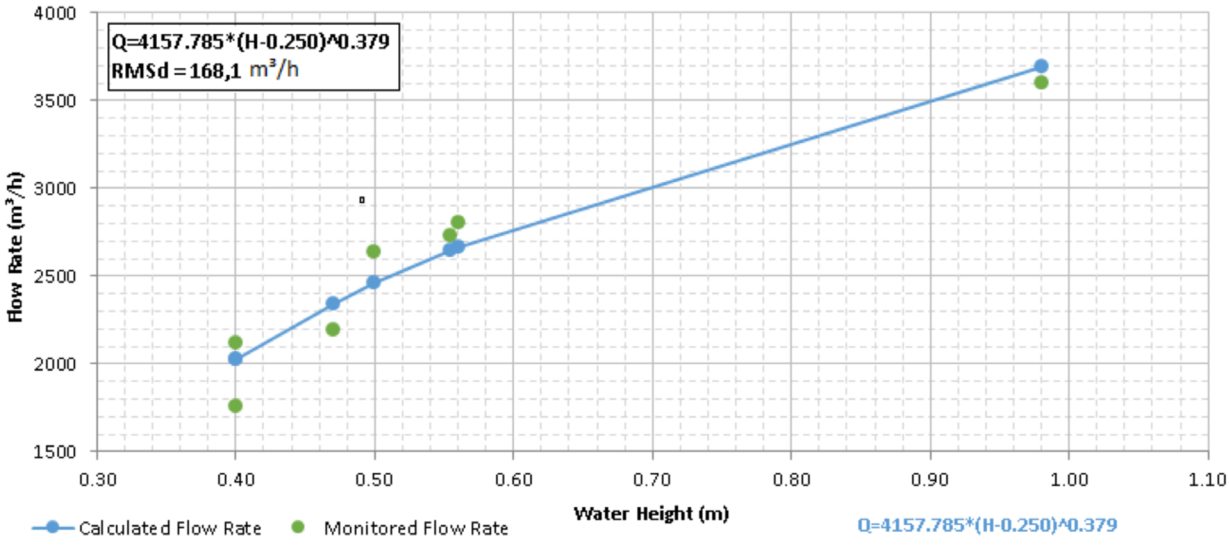

Figure 4C. Rating curve of Jaguara stream: calculated and monitored discharge.

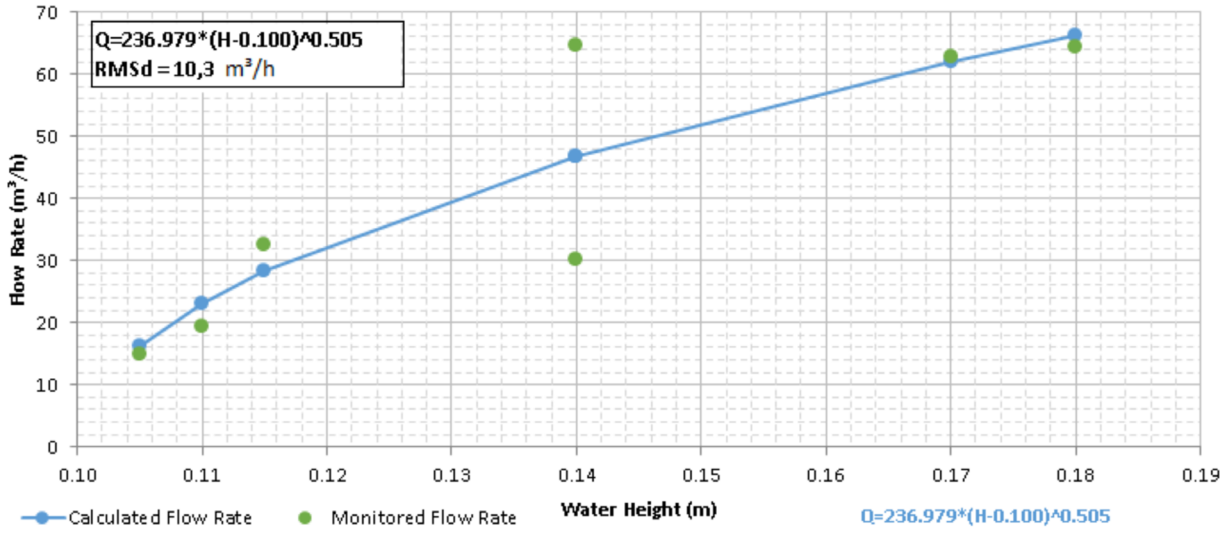

Figure 4D. Rating curve of Palmeiras stream: calculated and monitored discharge.

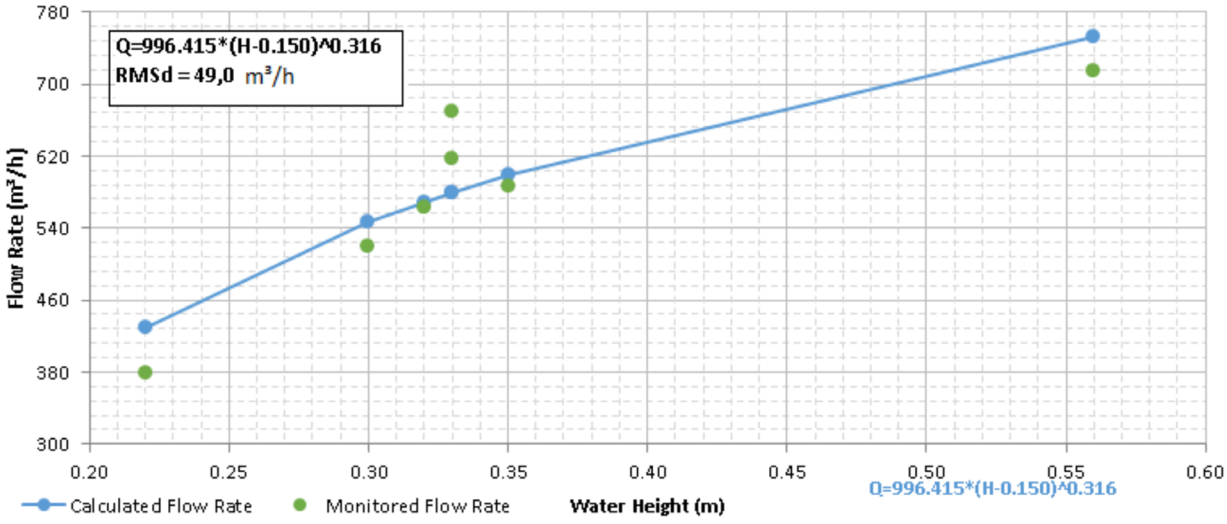

Figure 4E. Rating curve of Samambaia stream: calculated and monitored discharge.

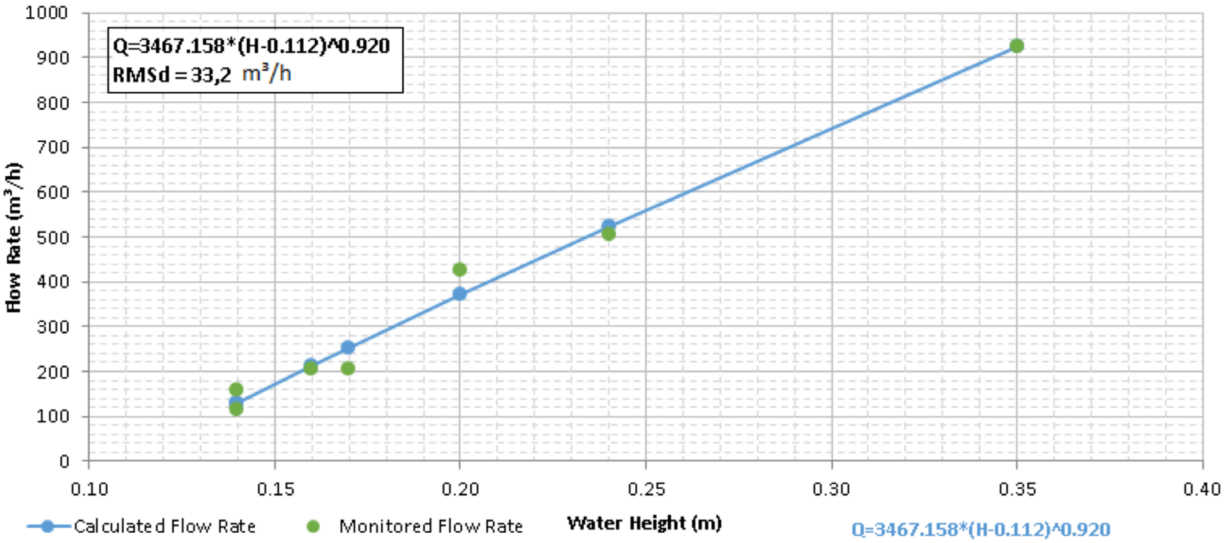

Figure 4F. Rating curve of Jaque stream: calculated and monitored discharge.

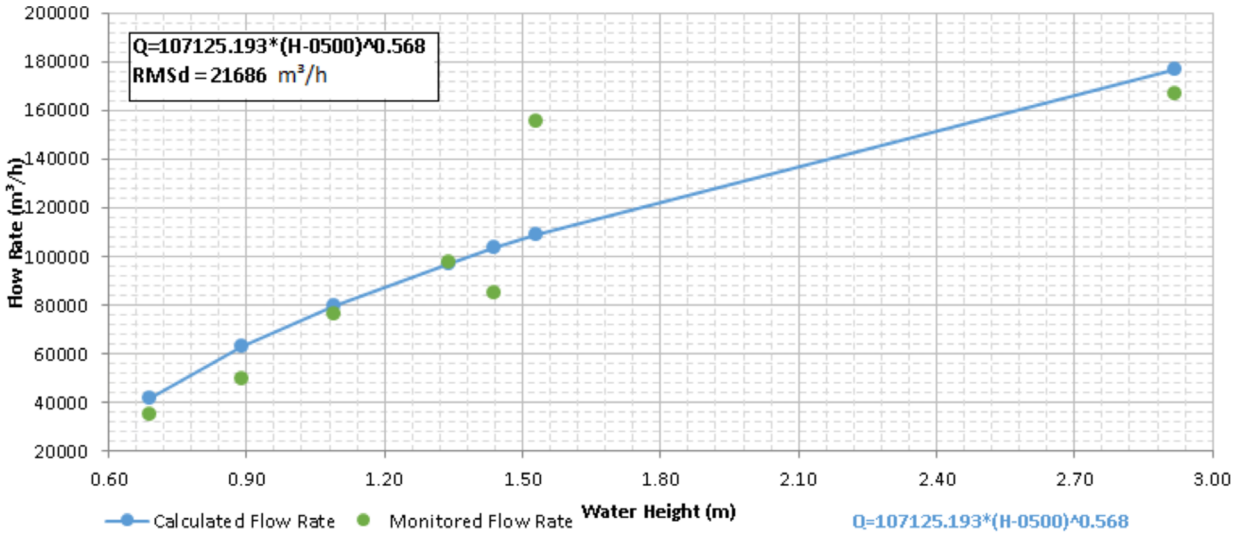

Figure 4G. Rating curve of the Velhas river: calculated and monitored discharge.

rate time series (Eqs. 3 and 5) were evaluated using the autocorrelation analysis (Fig. 5), as well as the cross-correlation flow rate (Fig. 6) with pluviometry. As proposed by Ferrari and Karmann (2008) and observed in Figures 5 and 6, the system loses memory between r(k) 0.1 and 0.2, in a karstic environment, changing the rating curve behavior and therefore no longer representing a cause-effect correlation. The temporal response relationship for autocorrelation (Fig. 5) and cross-correlation (Fig. 6) will be evaluated between the proposed interval of r(k), where the cause-effect relationship is still maintained. In other words, where the flow rate data are still correlatable in this interval (Fig. 5) as rain interferes with the flow response (Fig. 6).

The presented autocorrelation data is indicative of a maximum lag of two days for the Gordura, Jaguara, and Flor streams; three days for the Palmeiras stream; four days for the Jaque and Samambaia streams, and also the Velhas river. The higher values found for the Velhas river and Jaque stream may be related to the fact that these water bodies are not located exclusively in carbonate terrain. As for the Samambaia stream, the regularization of its ground-water flow is responsible for the slower flow response to precipitation.

The others presented greater values from 1 to 3 days in relation to the return time. Overall, the results are expressions of a well–developed karstic system and low fast ground-water flow storage.

The cross-correlation result (Fig. 6) shows a one–day response to the Gordura, Jaguara, Palmeiras, and Samambaia streams; two days for the Jaque and Flor stream; and three days for Velhas river.

The higher delay times found for the Velhas river may be related to the fact that it is not located exclusively on carbonate terrain and that contribution from other river systems exists external to the studied area. The slower response identified in the Jaque stream may be related to its predominantly pelitic geology. The Flor stream is being affected by the catchment present in its extension. The other basins, predominantly in karst terrains, presented an immediate response to rainfall events, as well as a very short system memory effect indicating a fast recharge for the underground system and high hydraulic conductivity.

Cause and effect data for the Gordura stream were close to 24 hours (Fig. 6). In order to test the adherence of the mathematical method to calculate the return time proposed by Ferrari and Karmann (2008), the results obtained for the Gordura stream were compared to the results found by Teodoro *et al.* (2019) in their tracer trials in the same basin. The former encountered a 23-hour delay between launch and reception of dye tracers in this basin. Thus, the efficiency of the method proposed by Ferrari and Karmann (2008) to estimate the travel time of a particle through the system can be evidenced.

Failure completion

The monitored and calculated hydrogram values were plotted together for comparison (Figs. 7A–7G). Pluviometry data corresponds to the station closest to the analyzed stream.

Since the goal is not only to complete the missing values but also to test the proposed methodology, the rating curves calculated and monitored during the hydrological year 2016/2017 were analyzed. For a better understanding, the data were evaluated according to drought and rainfall seasons, pluviometry events, sequential rains, high-intensity rainfall peaks, and anthropogenic interference whenever existing.

It was observed that during the dry season, from April to September, there is better adherence to the rating curve than during the rainy one. This phenomenon is probably due to a better response of discharge to pluviometric events without interference accumulation as a result of sequenced rainfall.

The calculated rating curves generally exhibit a slight shift to the right relative to the monitored values (Fig. 7). This occurs because the cross-correlation method was evaluated on a time scale of days. If the rainfall records were logged in hours (at the abscissa axis of the graphics in Fig. 7) it is certain that the time lag would be lower, thus the displacement between

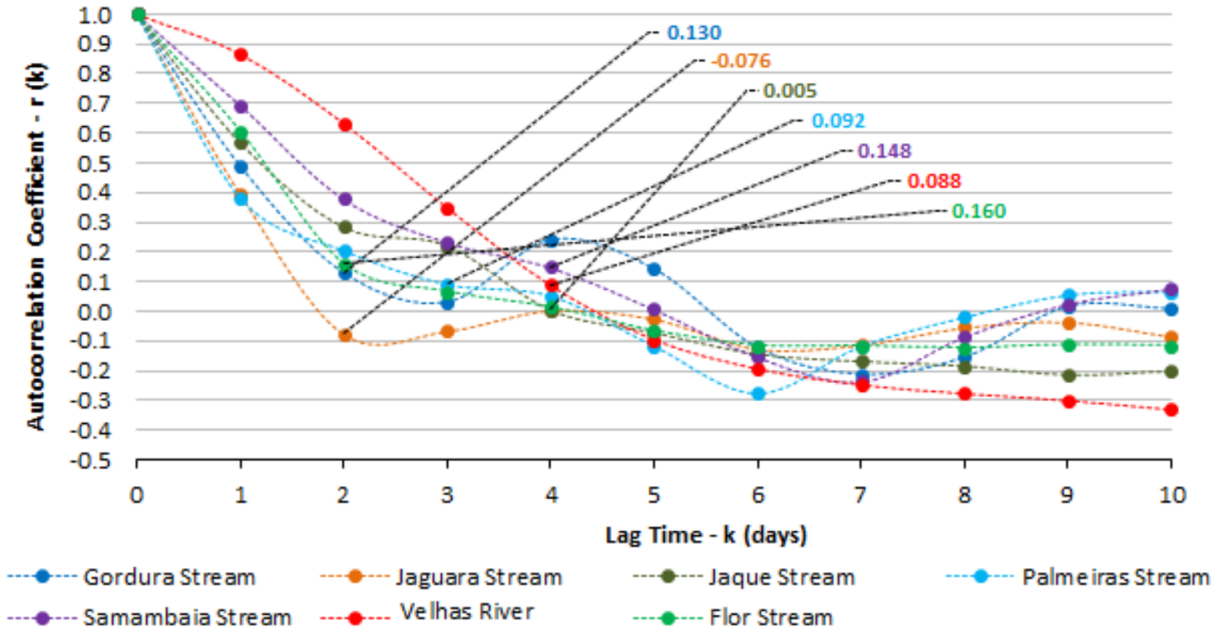

Figure 5. Flow rate data autocorrelation, where k(k) between 0.1 and 0.2 is representative of the loss of system memory (final of the correlation between flow rate data).

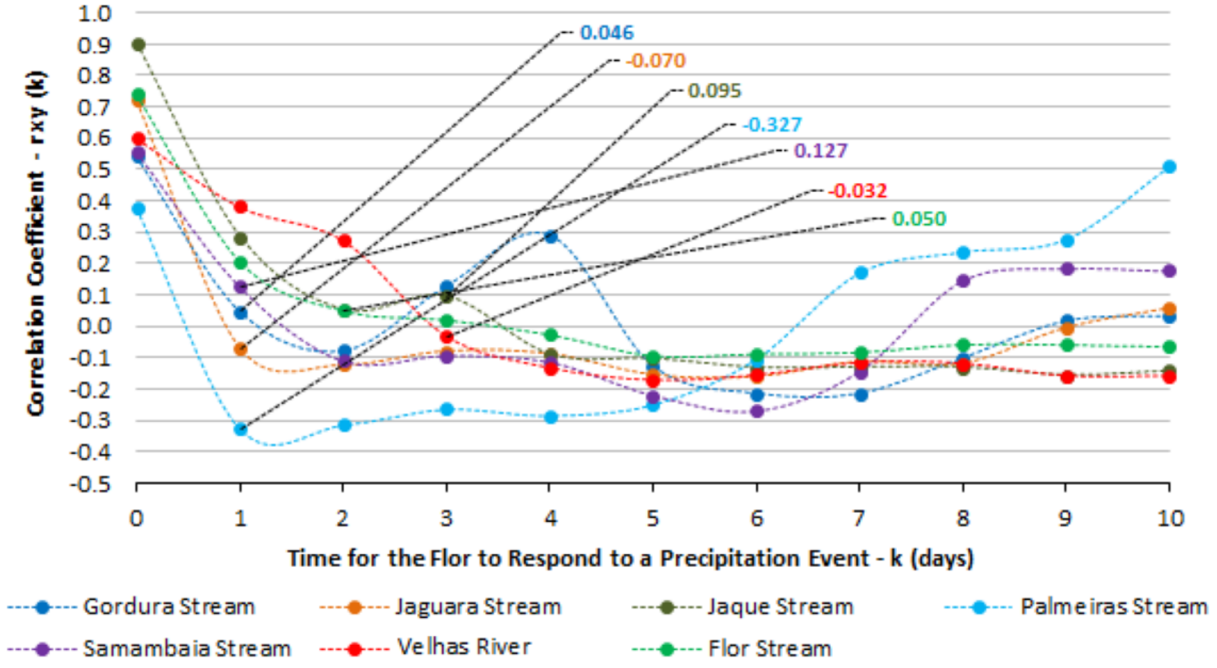

Figure 6. Cross-correlation between flow rate and rainfall data, where k(k) between 0.1 – 0.2 represents system memory loss (final influence of pluviometry on flow rate).

rating curves would be smoother and closer to the monitored and calculated rating curves.

In sequential rain events, the inclination of the rating curve is produced, enhancing periods of greater recharge. The geometry of the observed and calculated curves was very similar in shape, presenting excellent adherence to the methodological aspect and can also be used for flow rate separation and aquifer recharge calculations.

High-intensity rain spikes generated an instantaneous increase in discharge. For such cases, the calculated flow values are higher than the monitored ones. This happens because the calculated values react automatically to the daily pluviometry event, and despite the estimated surface runoff reduction (Eq. 8), this is perceived in units of days. The best fit for these variations would be to obtain hourly rainfall data so that the effect of Equation 8 would attenuate the calculated rating curve for hourly discharge events.

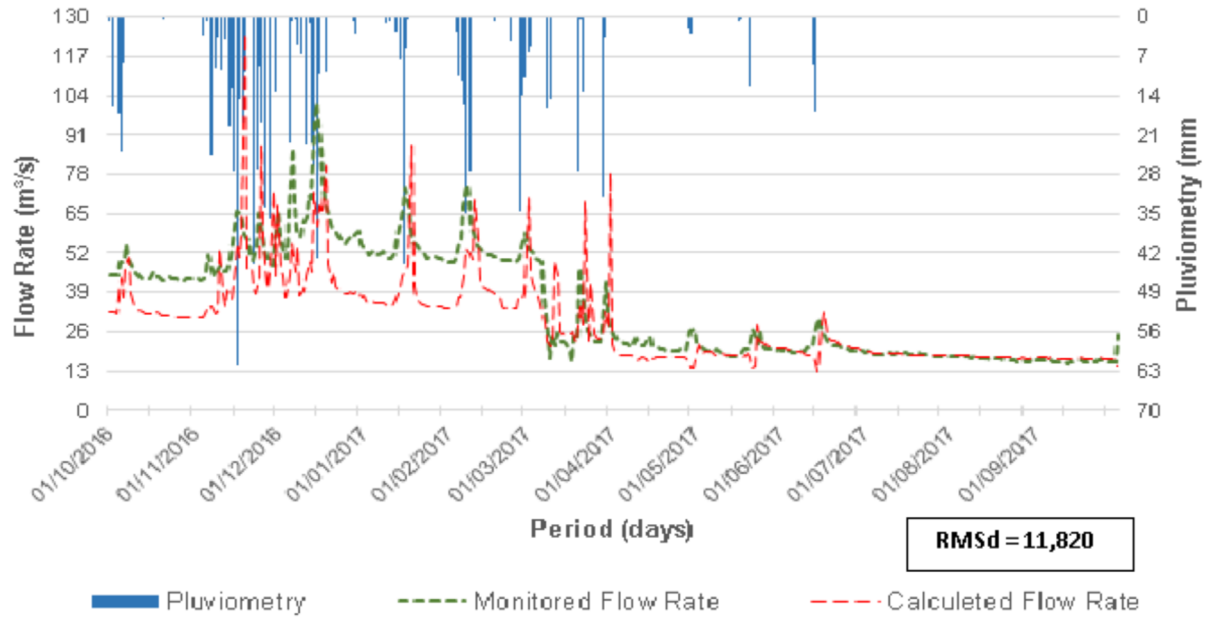

Figure 7A. Hydrograms of monitored and calculated streamflow rates of the Velhas river.

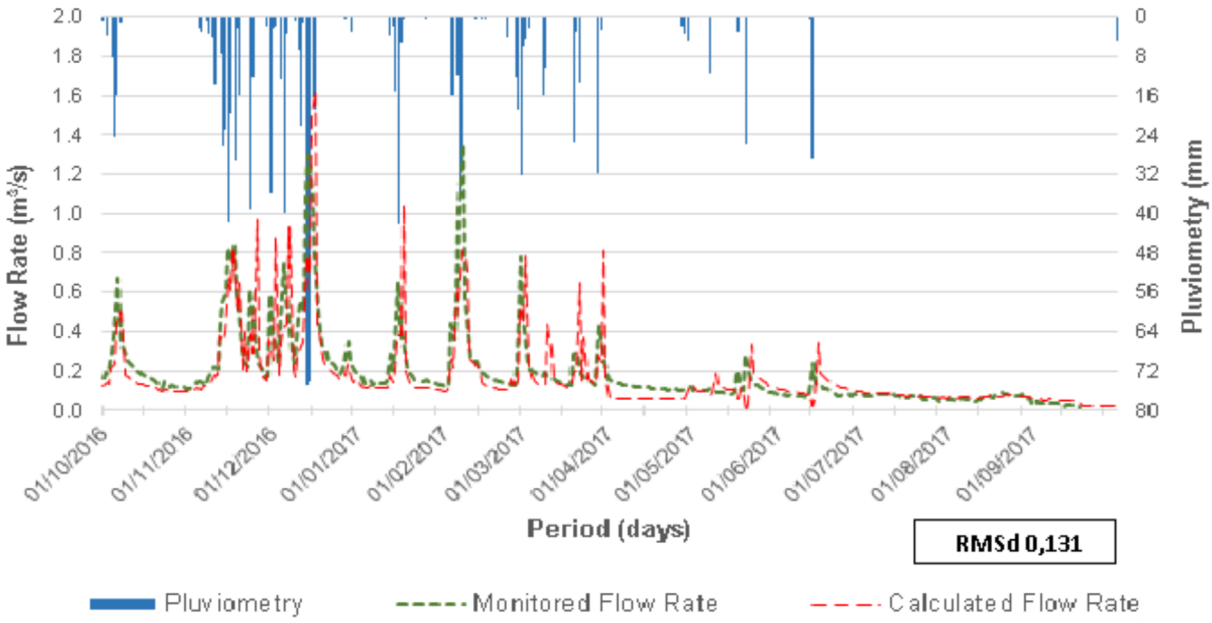

Figure 7B. Hydrograms of monitored and calculated Jaque streamflow rates.

The Velhas river dataset (Fig. 7A) had no missing values during the monitoring process. In the rainy season, a calculated curve shift below the monitored curve is observed, which is likely due to the size of the Velhas river basin and other pluviometric and fluviometric contributions. The difference between the measured and calculated annual volume per registration day was approximately 18.3% for the year and 1.7% for the dry period.

The Jaque stream (Fig. 7B) presented a minor monitoring failure at the end of September 2017. The difference between the annual volume measured and calculated per recording day was approximately 10.6% for the year and 5.6% for the dry period.

The Jaguara stream (Fig. 7C) presented monitoring failure between August and September 2017. The difference between the measured and calculated annual volumes was less than 2% for the analyzed hydrological year. The volume of water produced by rainfall events is not reflected in the measured flow rate (green curve) which is attributed to the contribution of deeper waters for this stream.

The Gordura stream (Fig. 7D) presented a period of monitoring failure in the transition between the rainy and dry periods (February and June 2017) with a difference between the measured and calculated annual volume of approximately 6.5% for the year and 1.7% for the dry season.

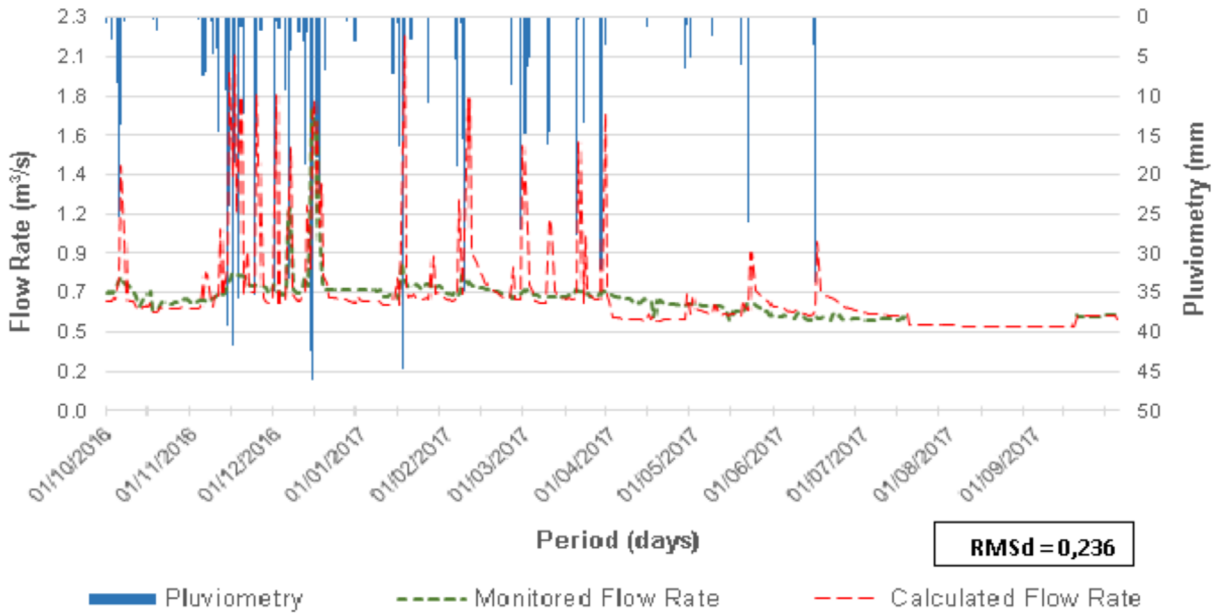

Figure 7C. Hydrograms of monitored and calculated Jaguara streamflow rates.

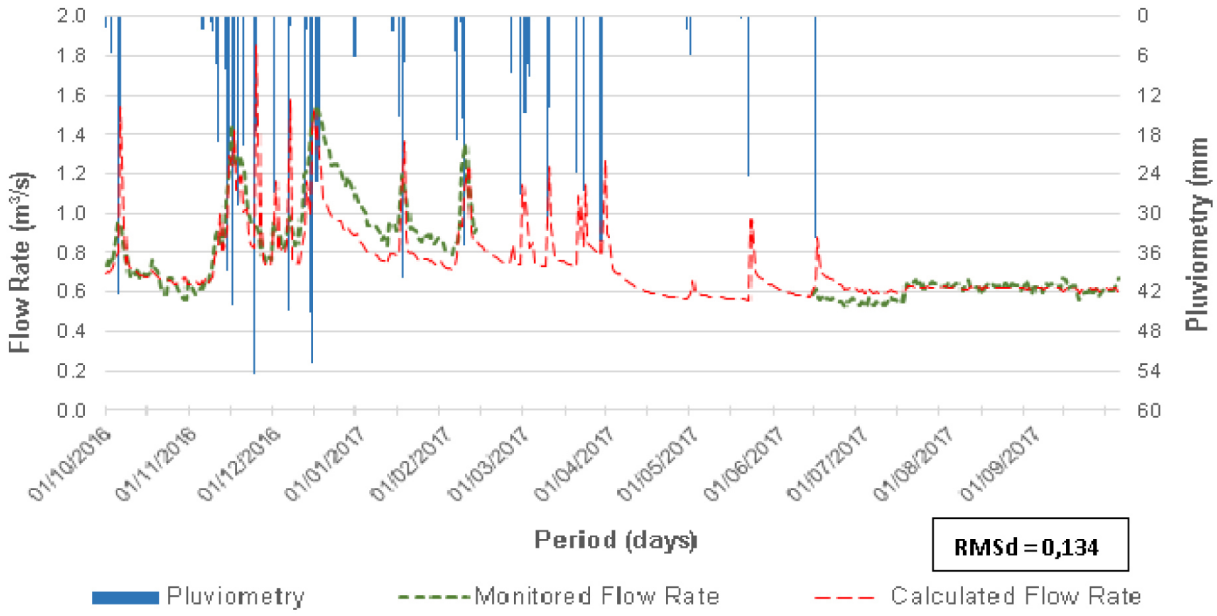

Figure 7D. Hydrograms of monitored and calculated Gordura stream flow rates.

The Samambaia stream (Fig. 7E) presented two periods of monitoring errors. The first, from October to December 2016 is represented by a pressure transducer operating error in the pressure transducer, which recorded only the same value. The second, from July to September 2017 represents a data collection failure, from the end of the rainy to the beginning of the dry period, displaying a downward displacement of the calculated rating curve when compared to the monitored one. This is due to the effect of flow rate regularization attributed to a dam located upstream to the monitoring point. It is supported by the fact that the recession began only in July, unlike other basins analyzed in the region. The difference between the monitored and calculated annual volume per record day was approximately 5%.

The Palmeiras stream (Fig. 7F) showed a period of monitoring failure between October and December 2016 and August and September 2017.

Despite the consistency of the calculated data in relation to rainfall events, there are divergences recorded in the dry season.

As there are more than 15 km between the fluviometric and rainfall stations, there are some periods during rainy season where recorded rain events did not lead to increased monitored water levels. This is attributed to the rainfall event not occurring over the basin area and as a consequence, there

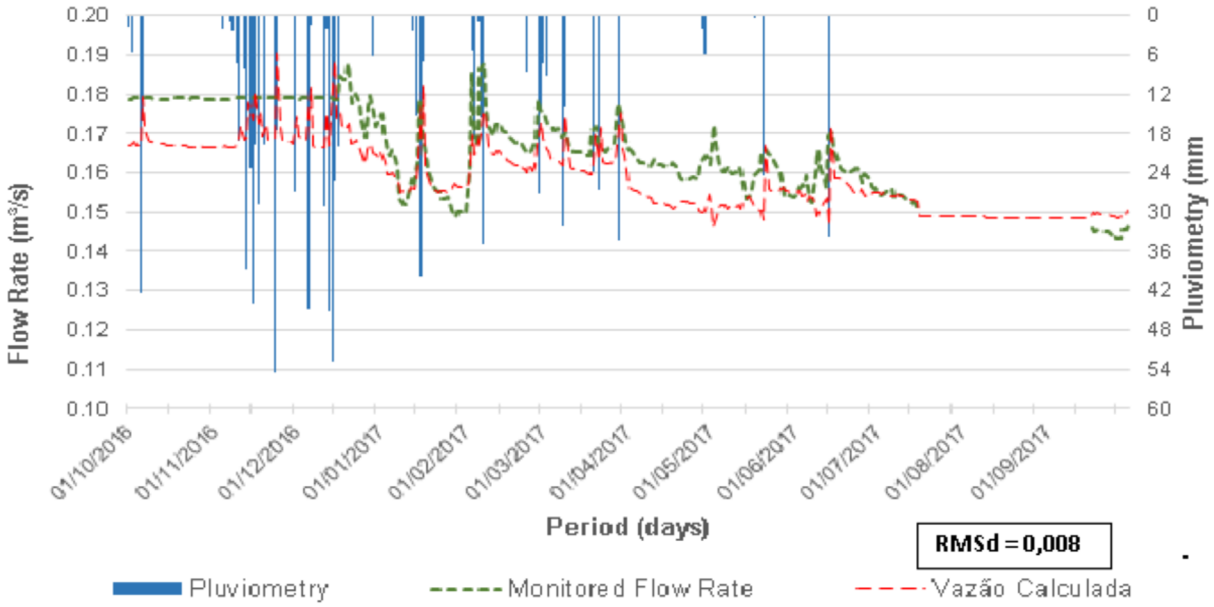

Figure 7E. Hydrograms of monitored and calculated Samambaia streamflow rates.

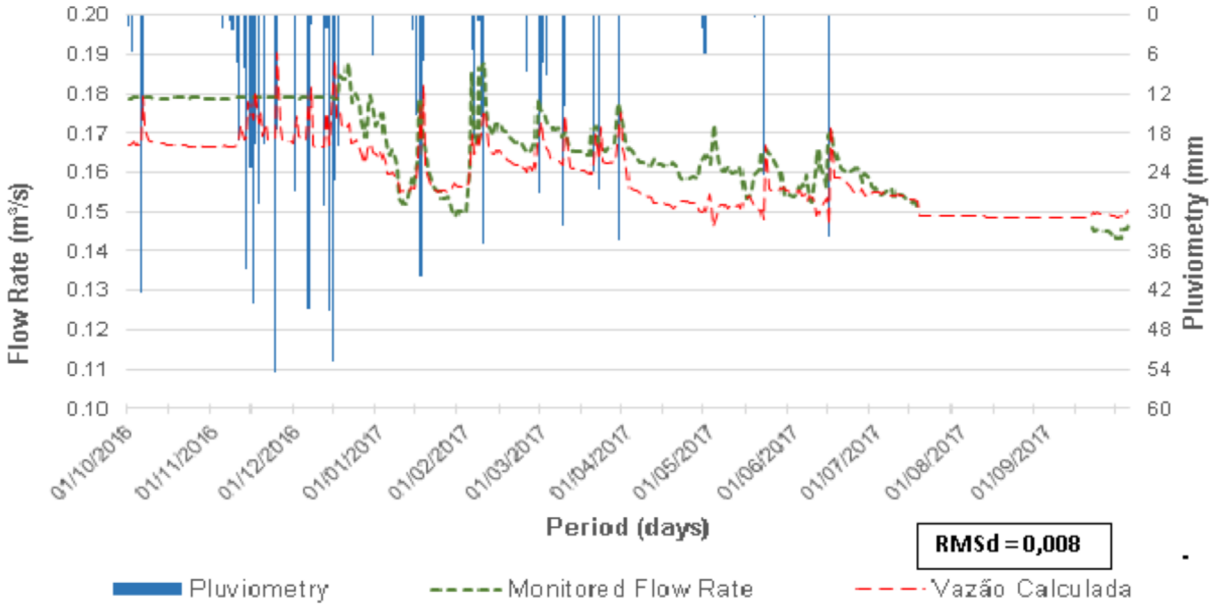

Figure 7F. Hydrograms of monitored and calculated streamflow rate for Palmeiras stream.

was no increase in the streamflow calculated through its rating curve. The pressure transducer records showed no errors, as there was a considerable reduction in the calculated values happening since the beginning of the dry period and there is no considerable variation in the monitored values (which happens in the other basins of the studied area). In a short period, from January to April 2017, when the monitored pluviometry and fluviometry data are more consistent, the difference between annual volumes was approximately 6.3%.

The Flor stream (Fig. 7G) presented a period of monitoring failure during most of the rainy season and the beginning of the dry one. The low streamflow monitored between June and July 2017 is related to the strong catchments identified in this stream. In a short period, from June to September 2017, where there is a correspondence of calculated and monitored data, the difference between annual volumes was approximately 8.2%.

The developed methodology presented an excellent adherence between calculated and observed data when comparing the different pluviometric and fluviometric situations in the basins, which are not correlated to anthropic interference. The difference between calculated and observed values was less than 9% for the hydrological year and less than 4% in the dry season. The mean square error shows satisfactory results for the Samambaia, Gordura, Jaguara, and Jaque basins. The other

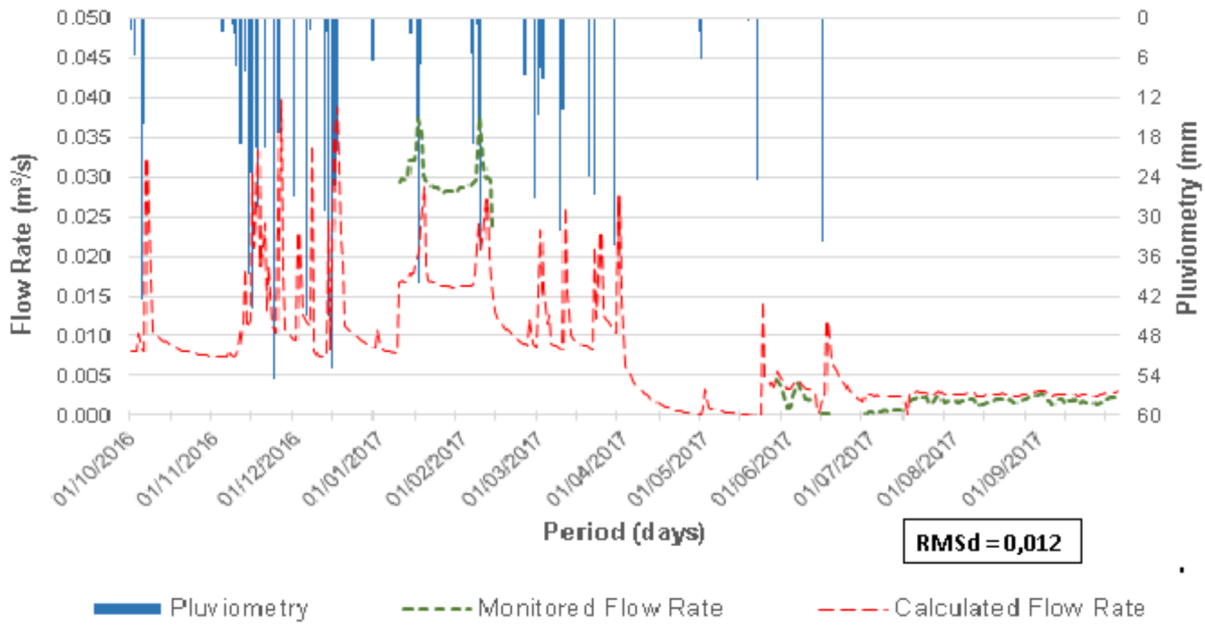

Figure 7G. Hydrograms of the monitored and calculated flow rates of the Flor stream.

basins presented higher normalized root mean squared nRMS, probably due to the calibration of the rating curve and interference present in these basins.

CONCLUSION

The rating curve data showed a good adherence between the calculated and measured values, and it is possible to apply these equations for the hydrological year 2016/2017 to obtain flow rates in this area. To continue using such curves, one should update the percentage deviations on an annual basis. The curve should be calibrated to maintain the error of less than 10%. Despite presenting percentage deviations lower than 10%, a larger number of points are required in order to reevaluate the mean square error For the Velhas river and Flor and Palmeiras stream curves.

The correlation results indicate an aquifer system with a fast and well-evolved ground-water flow controlled by conduits and, consequently, with low storage values. This is supported by the correlation coefficients, and cross-correlation ranging from 1 to 4 days, highlighting rapid responses of the underground system water level to rainfall events.

The methodology developed for the completion of time data in correlated series proved to be efficient as long as no anthropic or outside interference occurs to the evaluated system. This is exemplified by the Velhas river in relation to the extension of its basin. Also, by Flor and Palmeiras streams that are impacted by water withdrawals by catchments beyond and by the distance between the fluviometric and pluviometric stations, as seen in the Palmeiras stream basin. It was not possible to establish the distance relationship between the rainfall measurement point and streamflow, as it is controlled by nature factors. Therefore, it is recommended that pluviometric and fluviometric stations be installed near these points, in order to improve data quality.

The shape of the calculated rating curve fitted to the monitored curve showed good adherence, presenting some deviations regarding the responses of the correlation events or the quality of the rating curve used. Because it is a mathematical–based methodology compared with natural events, the deviations of less than 10% (for analyzes in which no anthropic or other interference has occurred) show an adequate method to be used in carbonate basins.

Therefore, for correlated coefficients, the use of the fill–in method is reliable and useful for time series, especially for small basins, since in large basins the chances of interferences occurring at more than one point are greater.

Finally, it is important to emphasize that the method was developed for only one hydrological year. Available data over longer periods may increase the precision of the results. For future studies, it is recommended to apply the proposed methodology to longer periods, as well as in other correlated systems such as groundwater level, pluviometry, flow rate, and non-carbonate terrain, aiming to validate the method in other areas or geological contexts.

ACKNOWLEDGMENTS

To the Gerdau Group for supporting researches of the Process Project FUNDEP/GERDAU/UFMG No. 22.317, to the National Center for Research and Conservation of Caves (*Centro Nacional de Pesquisa e Conservação de Cavernas* — CECAV), and FAPEMIG (APQ— 02049-14) for financial support, to the Geosciences Institute of the Universidade Federal de Minas Gerais, to the Nuclear Technology Development Center (*Centro de Desenvolvimento de Tecnologia Nuclear* — CDTN), to the Geological Service of Brazil (*Serviço Geológico do Brasil* — CPRM) and to the Minas Gerais Institute for Water Management (*Instituto Mineiro de Gestão das Águas* — IGAM) for their participation and support during all the stages.

ARTICLE INFORMATION
Manuscript ID: 20190031. Received on: 05/07/2019. Approved on: 07/11/2020.
R.P. wrote the article developing the chapters of introduction, physical characteristics of the study area, materials and methods, results and discussion, and conclusion. Also, he took part in the revision process of the abstract, as well as in bibliographic references. L.V. wrote the abstract, participated in the mathematical development contained in the materials and methods chapter, and reviewed and contributed to other parts of the article.
Competing interests: The authors declare no competing interests.

REFERENCES

Andrade I.B., Amorim J.B. 2018. *Mapeamento geológico com ênfase na relação hidráulica entre o complexo granítico–gnáissico com o grupo Bambuí.* Graduation Work, Universidade Federal de Minas Gerais, Belo Horizonte, 105 p.

Auler A. 1994. *Hydrogeological and Hydrochemical Characterization of the Matozinhos–Pedro Leopoldo Karst, Brazil.* Msc Thesis, Faculty of the Department of Geography and Geology, Western Kentucky University, Bowling Green, 110 p.

Barbosa S.E.S. 2004. *Análise de dados Hidrológicos e Regionalização de Vazão da Bacia do Rio do Carmo*. Master Dissertation, Núcleo de Pesquisa em Recursos Hídricos, Universidade Federal de Ouro Preto, Ouro Preto, 211 p.

Collischonn W., Tassi R. 2008. *Introduzindo a Hidrologia.* Instituto de Pesquisas Hidráulicas, Universidade Federal do Rio Grande do Sul, Porto Alegre, 274 p.

Ferrari J.A., Karmann I. 2008. Comportamento Hidrodinâmico de Sistemas Cásticos na Bacia do Rio Betari, Município de Iporanga – SP. Paulo, SP. *Revista do Instituto de Geociências da Universidade de São Paulo*, **8**(1):1-13. https://doi.org/10.5327/Z1519-874x2008000100001

Freund R.J., Wilson W.J. 1998. Regression Analysis: Statistical Modeling of a Response Variable. San Diego: Academic Press Technometrics. v. 17. 368 p.

Galvão P., Hirata R., Cordeiro A., Barbati D., Peñaranda J. 2016. Geologic conceptual model of the municipality of Sete Lagoas (MG, Brazil) and the surroundings. *Anais da Academia Brasileira de Ciências*, **88**(1):35-53. http://dx.doi.org/10.1590/0001-3765201520140400

Obregon E., Tucci C.E.M., Goldenfum J.A. 1999. Regionalização de Vazão com Base em Séries Estendidas: Bacias Afluentes à Lagoa Mirim, RS. *Revista Brasileira de Recursos Hídricos*, **4**(1):57-75. http://dx.doi.org/10.21168/rbrh.v4n1.p57-75

Paula R.S. 2019. *Modelo Conceitual Modelo Conceitual de Fluxo dos Aquíferos Pelíticos – Carbonáticos da Região da APA Cárstica de Lagoa Santa, MG*. Doctoral Thesis, Universidade Federal de Minas Gerais, Belo Horizonte, 272 p.

Paula R.S., Velásquez L.N.M. 2019. Balanço Hídrico em Sistema Hidrogeológico Cárstico de Lagoa Santa, Minas Gerais. *Águas Subterrâneas*, **33**(2):119-133. https://doi.org/10.14295/ras.v33i2.29252

Pessoa P.F.P. 2005. *Hidrogeologia do aquífero cárstico coberto de Lagoa Santa, MG*. Doctoral Thesis, Universidade Federal de Minas Gerais, Belo Horizonte, 375 p.

Piscoya R.C.C.C., Lopes W.T.A., Lemos G.M., Silva L.S., Silva M.C.A.M. 2013. Análise de consistência de dados fluviométricos de estações de monitoramento da ANA localizadas nas sub–bacias hidrográficas 10 (rios Solimões, Javari e Itaquaí) e 11 (rios Solimões, Içá e Jandiatuba). *In*: Simpósio Brasileiro de Recursos Hídricos, Bento Gonçalves, 2013. *Anais...* Associação Brasileira de Recursos Hídricos. p. 1-8.

Ribeiro C.G., Velásquez L.N.M., Paula R.S., Meireles C.G., Lopes N.H.B., Arcos R.E.C., Amaral D.G.P. 2019. Análise dos fluxos nos aquíferos cárstico–fissurais da região da APA Carste de Lagoa Santa, MG. *Águas Subterrâneas*, **33**(1):12-21. https://doi.org/10.14295/ras.v33i1.29148

Ribeiro J.H., Tuller M.P., Filho A.D., Padilha A.V., Córdoba C.V. 2003. *Projeto VIDA:* Mapeamento geológico, região de Sete Lagoas, Pedro Leopoldo, Matozinhos, Lagoa Santa, Vespasiano, Campim Branco, Prudente de Morais, Confins e Funilândia, Minas Gerais – relatório final, escala 1:50.000. 2. ed. Belo Horizonte: CPRM, 54 p.

Rolim G.S., Sentelhas P.C., Barbieri V. 1998. Planilhas no ambiente EXCEL para os cálculos de balanços hídricos: normal, sequencial, de cultura e de produtividade real e potencial. *Revista Brasileira de Agrometeorologia*, **6**(1):133-137.

Tamiosso M.F., Tamiosso C.F., Araújo R.K., Cruz J.C., Horn J.F.C., Silva R.L.L., Pascotini P.B., Perotto F. 2013. Preenchimento de Falhas de dados Observados de Vazão Utilizando a Equação de Manning. *In*: Simpósio Brasileiro de Recursos Hídricos, 20., 2013. *Anais...* p. 1-8.

Teodoro M.I.P., Velásquez L.N.M., Fleming P.M., Paula R.S., Souza R.T., Doi B.B. 2019. Hidrodinâmica do Sistema Aquífero Cárstico Bambuí, com uso de Traçadores Corantes, na Região de Lagoa Santa, Minas Gerais. *Águas Subterrâneas*, **33**(4):392-406. https://doi.org/10.14295/ras.v33i4.29532

Thornthwaite C.W. 1948. An approach toward a rational classification of climate. *Geogr. Rev*, **38**(1):55-94. https://doi.org/10.2307/210739

Vieira H.S., Kohler H.C., Tavares V.P. (Eds.). 1998. *APA Carste de Lagoa Santa – Meio Físico*. Belo Horizonte: IBAMA/CPRM, 301 p. v. 1.

Zahed Filho K., Silva R.M., Porto R.L.L. 2001. *Medição de Vazão e Curva Chave*. PhD, Departamento de Engenharia Hidráulica e Sanitária, Escola Politécnica da Universidade de São Paulo, São Paulo, 48 p.